

Polyaniline/TiO₂/kaolinite: the composite material with high electrical anisotropy

Jonáš Tokarský^{a*}, Lucie Neuwirthová^a, Pavlína Peikertová^a, Lenka Kulhánková^{a,b}, Kateřina Mamulová Kutlákova^a, Vlastimil Matějka^a, Pavla Čapková^c

^a Nanotechnology Centre, VŠB – Technical University of Ostrava, 17. listopadu 15, 708 33 Ostrava, Czech Republic.

^b Faculty of Metallurgy and Materials Engineering, VŠB – Technical University of Ostrava, 17. listopadu 15, 708 33 Ostrava, Czech Republic.

^c Faculty of Science, J. E. Purkyně University, České mládeže 8, 400 96 Ústí nad Labem, Czech Republic.

Abstract

Kaolinite-TiO₂ nanocomposite matrix (KATI) coated with polyaniline (PANI) layer has been prepared in powder form and pressed into tablets. The conductivity was studied in dependence on (1) wt.% of TiO₂ in KATI matrix and (2) thermal pre-treatment of KATI matrix. The anisotropy factor α , i.e. the ratio of in-plane conductivity and conductivity in the direction perpendicular to the tablet plane, was found to be very high for PANI/KATI tablet (α is of the order of $10^3 - 10^4$) in comparison with pure PANI tablet (α is of the order of 10^2). Structure has been studied using Raman spectroscopy, X-ray diffraction analysis, scanning electron microscopy and molecular modeling. The possibility of using the tablets as a load sensors have been tested and tablets pressed from composites containing calcined KATI seem to be promising material for this purpose.

Keywords:

A. composite materials;

B. chemical synthesis;

C. computer modelling and simulation;

D. electrical conductivity

* Corresponding author

Address: Nanotechnology Centre, VŠB – Technical University of Ostrava, 17. listopadu 15, 70833 Ostrava, Czech Republic.

1. Introduction

Polyaniline (PANI), the most intensively studied conducting polymer, may exist in many oxidation and protonation states. The common green protonated emeraldine salt, formed during the polymerization of aniline in acidic environment, exhibits conductivity on a semiconductor level [1]. The conductivity is caused by polaronic structure which can be easily determined using Raman spectroscopy [2,3]

Nanocomposites based on PANI are studied and used in wide range of applications, like sensors, energy storage systems, electrostatic discharge protection materials, electrorheological fluids, and many others [4,5]. Ordering of polymer chains plays a key role

in these systems [6-16]. PANI chains can be aligned, for example, using high pressure [17], blends with insulating polymers [13], mechanical orientation of PANI films [14], ordering of PANI particles in monomer mixture in an electric field [15]. Nanocomposites of PANI/layered inorganic matrix type (i.e. PANI/graphite [11] or PANI/phyllosilicate [18-21]) offer another possibility how to order the PANI chains along platy particles of layered matrices. In addition, the interaction between PANI chains and matrices improves and gives rise to properties, such as mechanical and thermal stability [19] or photosensitivity [22]. For a comprehensive review the reader is referred to [4].

Clay minerals with the layered structure (phyllosilicates) have been often used as matrices for such type of organo-inorganic composites [23-25]. The plate-like shape of phyllosilicate particles remains unchanged even after the surface modification and the powder particles of resulting nanocomposites exhibit the tendency to preferred arrangement even without any applied pressure. Therefore, pressing these nanocomposites into the tablets using high pressure will lead to a strong texture dramatically affecting the conductivity.

Although the design of functional units based on these nanocomposites has to take into account this effect of texture, only few works focused on this topic can be found [7,26]. In the majority of articles dealing with the conductivity of tablets pressed from PANI/phyllosilicate composites the anisotropy is not discussed [17,18,27-30]. Moreover, the most used phyllosilicate in these works is the montmorillonite. Kaolinite (KLT) as a matrix for PANI is described only by Duran et al. [19], while Anakh and Çetinkaya [31] and Acar et al. [32] used KLT for the preparation of poly(2-ethyl aniline)/KLT and polypyrrole/KLT composites, respectively.

Present work is focused on structure and electrical conductivity of tablets pressed from PANI/KLT and PANI/KATI composites, where KATI means KLT covered by TiO₂ nanoparticles [33]. Raman spectroscopy, scanning electron microscopy, X-ray diffraction analysis and molecular modeling are used to study the structure of composites. The electrical conductivity is studied in dependence on thermal pre-treatment of KATI and amount of TiO₂ in KATI. The anisotropy factor α (i.e. the ratio of in-plane conductivity and conductivity in the direction perpendicular to the tablet plane) is determined for each sample. A possibility of using the tablets as a load sensors is also discussed.

2. Materials and methods

2.1 Samples preparation

Kaolinite/TiO₂ composites (KATI) were prepared from kaolinite SAK47 (Lasselsberger a.s.) with titanyl sulfate as a precursor. Samples denoted as KATI1X are composites dried at 105 °C and symbol X means the content of TiO₂ (2 for 20 wt.%, 4 for 40 wt.%, 6 for 60 wt.%). Samples denoted as KATI6X were calcined at 600 °C and meaning of the symbol X is the same as in KATI1X. More information about preparation of the composites can be found in [33].

Aniline, sulfuric acid and ammonium peroxodisulfate were purchased from Lach-Ner, Czech Republic, and used as received. PANI powder was prepared by oxidative polymerization of the solution of aniline by ammonium peroxodisulfate in acidic environment (sulfuric acid). Time of the polymerization was 40 minutes (dark green color was observed). The solid was collected on a filter by rinsing with distilled water and subsequently dried at 40 °C in a kiln.

PANI/KATI1X, PANI/KATI6X and PANI/KLT composites were prepared using one-step process [28]. The anilinium sulfate and ammonium peroxodisulfate were added into water suspension containing 3 g of either KATI or KLT matrix. Polymerization of aniline was completed after 40 minutes, but the suspension was stirred for 6 hours. The solid was also collected on a filter by rinsing with distilled water and dried at same conditions as pure PANI. Prepared composites were pressed into tablets using LECO hand press (applied pressure 28 MPa) at room temperature, without any lubrication and binder. Diameter of each tablet was 32 mm. Thicknesses of PANI/KATI (both 1X and 6X), PANI and PANI/KLT tablets were 3.0 - 3.2 mm, 3.8 mm and 2.8 mm, respectively. Weight fraction of PANI in each sample calculated according to Duran et al. [19] is 27 wt.%.

2.2. Conductivity measurements

Two pairs of Cu contact electrodes have been used for the measurements of electrical conductivity in two perpendicular directions. Electrodes in each pair had different shape (see Fig. 1). Measuring instruments: DC POWER SUPPLY HY 5 3003 D-2, Programmable DC POWER SUPPLY BK PRECISION 9120, multimeter AGILENT 34401A, V-meter UNI-T UT802, pA-meter KEITHLEY 6487. Voltage $U = 1$ V was used for all measurements.

For the measurement of conductivity in the direction parallel to the round surface of pressed tablet (i.e. conductivity in the direction perpendicular to the direction of pressing, see Fig. 1),

the tablet was placed between two curved electrodes. Each conductivity measurement was repeated four times. Then, the tablet was rotated about 90° and the measurement was again repeated four times. The conductivity value for each sample is presented as an average value obtained from all eight measurements.

The dependence of electrical current flowing through the tablet in the direction perpendicular to the round surface of tablet (i.e. in the direction of pressing, see Fig.1a) on mechanical load was used to study the possibility of using PANI/KATI tablets as load sensors. Twelve weights (124 g each) were used. Since the area of the round surface of tablet is $0.8 \cdot 10^{-3} \text{ m}^2$, each weight represents the pressure 1513 Pa. Experiment started after loading the tablet with two weights. Then, pairs of additional weights were added at definite time intervals (denoted as the loading part of measurement,). After reaching the maximum load (i.e. 1488 g or 18156 Pa), pairs of weights were again removed at the same time intervals (denoted as the unloading part of the measurement).

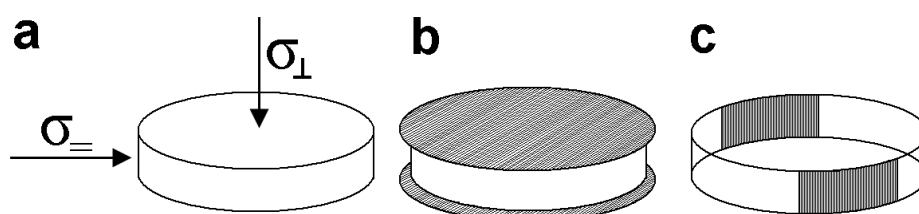


Fig. 1. (a) conductivities measured in the direction perpendicular and parallel to the flat round surface of tablet are denoted as σ_{\perp} and σ_{\parallel} , respectively; (b) flat round electrodes for σ_{\perp} measurement; (c) curved electrodes for σ_{\parallel} measurement.

2.3. Structure characterization

Smart Raman Microscopy System XploRATM (HORIBA Jobin Yvon, France) was used for the characterization of prepared samples. Raman spectra were acquired with 532 nm excitation laser source, with 50 \times objective and using 1200 gr./mm grating.

Images from the measurement on QUANTA 450 FEG (FEI) scanning electron microscope (SEM) were obtained using a secondary electron detector. Accelerating voltage used was 15 kV.

The X-ray diffraction patterns were recorded using Bruker D8 Advance diffractometer (Bruker AXS, Germany) equipped with fast position sensitive detector VÅNTEC 1. $\text{CoK}\alpha$ irradiation ($\lambda = 0.178897 \text{ nm}$) was used. Measurements of all samples were carried out in reflection mode in symmetrical Bragg-Brentano arrangement. In order to analyze the texture of tablets, diffraction patterns have been recorded from three diffraction planes defined by the

incident and diffracted beam: top round surface, outer curved surface and inner cutting surface. The inner cutting surface was carefully treated with brush before the measurements. Molecular modeling in Accelrys Materials Studio (*MS*) was used to study the interaction energies between PANI chains and various KLT and TiO₂ surfaces in order to determine which part of the KATI composite the PANI chains prefer. Seven models of KLT and TiO₂ (anatase form) surfaces have been prepared according to the structures published in [34,35] and denoted as KLT(001), KLT(100), TiO₂(001), TiO₂(100), TiO₂(101), TiO₂(103), and TiO₂(112). The numbers in parentheses represent the Miller indices (see Table 1). Models of TiO₂ substrates have been built with one side protonated in order to study the interaction between PANI and protonated or unprotonated surfaces. Taking into account that the highest conductivity is exhibited by PANI/KATI14 sample, only KLT and anatase structures were studied. Models of calcined samples containing rutile and dehydroxylated KLT (see [33]) were not prepared.

Table 1

Sizes and crystallochemical formulae of KLT and TiO₂ substrates. The numbers in parentheses represent the Miller indices.

substrate	size [nm]	crystallochemical formula
KLT(001)	5.1 × 5.4	Al ₂₄₀ Si ₂₄₀ O ₆₁₀ (OH) ₄₆₀
KLT (100)	5.2 × 5.2	Al ₂₃₈ Si ₂₅₂ O ₅₁₁ (OH) ₇₀₀
TiO ₂ (001)	4.9 × 4.9	Ti ₆₇₆ O ₁₂₄₇ (OH) ₂₁₀
TiO ₂ (100)	4.9 × 4.7	Ti ₅₆₇ O ₁₀₆₇ (OH) ₁₃₄
TiO ₂ (101)	4.9 × 4.9	Ti ₄₁₆ O ₇₈₀ (OH) ₁₀₄
TiO ₂ (103)	4.9 × 5.3	Ti ₃₆₃ O ₇₃₀ (OH) ₁₉₂
TiO ₂ (112)	4.8 × 4.9	Ti ₃₃₃ O ₅₈₁ (OH) ₁₇₀

Initial models were prepared by placing the PANI chains (chemical formula C₄₈ H₄₂ N₈, length ~ 4.0 nm [36]) on the above mentioned substrates in various positions. Models containing PANI on protonated TiO₂ surface are denoted as PANI/TiO₂(101)OH, PANI/TiO₂(103)OH, etc. Also the models with PANI situated on octahedral KLT surface are denoted as PANI/KLT(001)OH, while PANI/KLT(001) means the PANI chain on tetrahedral surface. PANI/KLT(100)OH model contains fully protonated KLT edge. In PANI/KLT(100) model the KLT edge sets the uncovered aluminium atoms to PANI chains.

Initial models were optimized in *MS Forcite* module using Universal force field [37]. Smart algorithm was used with 500.000 iteration steps. Charges of atoms in PANI chain were assigned by Gasteiger method [38]. Gast_polygraph 1.0 parameter set containing enhancements for the treatment of four-valent nitrogen was used. Charges of atoms in KLT

and TiO₂ substrates were calculated using QEq method (QEq_charged 1.1 parameter set) [39].

The interaction between the PANI chain and either KLT or TiO₂ substrate was quantified using the adhesion energy E_{ad} calculated from optimized models

$$E_{ad} = (E_{tot,PANI} + E_{tot, substrate}) - E_{tot} \quad (1)$$

where E_{tot} is the total potential energy of the model (i.e. PANI chain anchored on either KLT or TiO₂ substrate), $E_{tot,PANI}$ is the total potential energy of PANI chain and is $E_{tot,substrate}$ is the total potential energy of either KLT or TiO₂ substrate. These energies are expressed in the unit (kJ·mol⁻¹).

3. Results and discussion

3.1. Morphology of the materials

SEM analysis was used to study the morphology of prepared materials and the images can be seen in Figs. 2a-f.

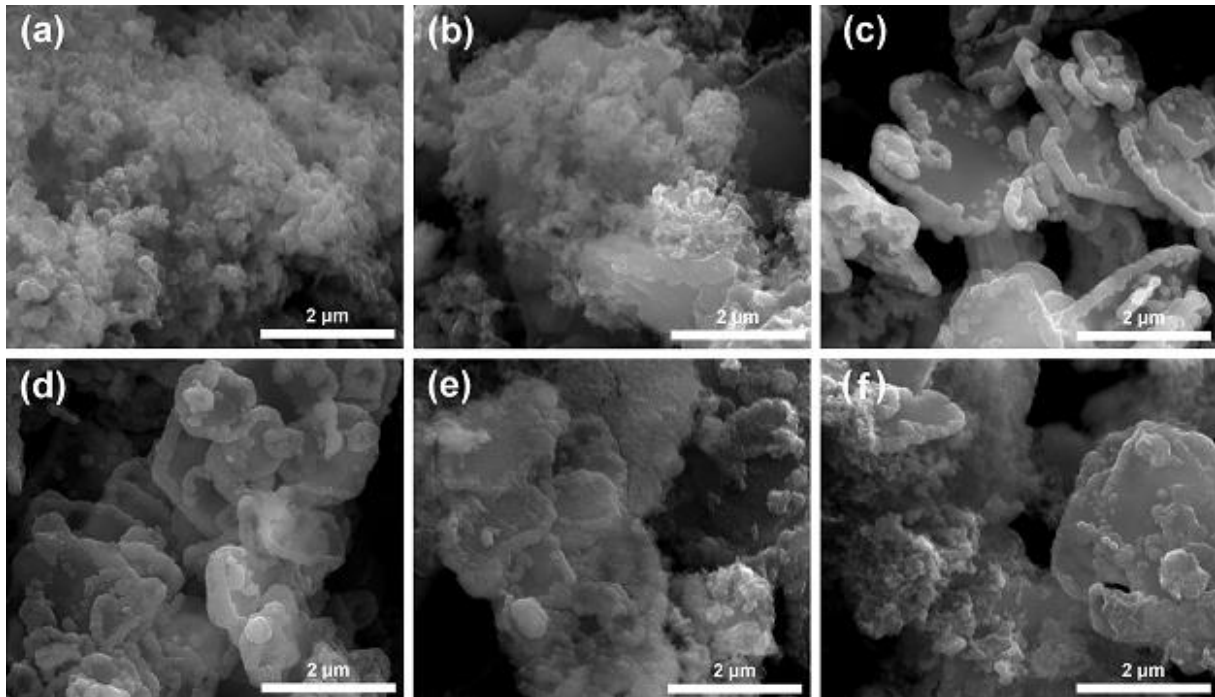


Fig. 2. (a) pure PANI – disordered clusters are formed; (b) PANI/KLT – PANI does not fully cover the KLT particles, see the plain KLT surface on the right; (c) pure KATI14 – “collars” from TiO₂ encircling the KLT particles are clearly visible; (d) pure KATI64 – the morphology of KATI14 is preserved but one can see cracks on TiO₂ “collars”; (e) PANI/KATI14 – KATI14 is fully covered by PANI; (f) PANI/KATI64 – coverage is not full, see the plain surface of KATI64 on the right.

Pure PANI and PANI/KLT composite can be seen in Figs. 2a and b, respectively. Fig. 2b reveals that KLT is not fully covered by PANI (see the plain KLT surface on the right). The structure of PANI in PANI/KLT composite is also very similar to that of pure PANI, i.e. disordered clusters composed from smaller beads (compare Figs. 2a and 2b). As same as in our previous study [33], the SEM images show that TiO₂ nanoparticles grow preferentially on KLT edges and create a “collars” encircling platy KLT particles (Figs. 2c-f). Fig. 2b shows that PANI grows also on the edges of pure KLT (see the upper part of image) but not preferentially. For PANI/KATI14 composite the SEM analysis revealed the complete coverage of KATI14 by PANI layer (Fig. 2e).

In order to determine the interactions between PANI and TiO₂ or KLT surfaces, the molecular modeling was involved also in this study. Adhesion energies (E_{ad}) for PANI chains on KLT and TiO₂ substrates calculated using *Eq. 1* are listed in Table 2.

Table 2

Adhesion energies PANI-substrate (E_{ad}) for various types of substrates in all optimized models. The first line contains E_{ad} for PANI on tetrahedral KLT (Si-O) and unprotonated TiO₂ (Ti-O) surfaces, the second line shows E_{ad} for octahedral KLT and protonated TiO₂ (OH) surfaces.

type of surface	PANI-substrate E_{ad} [kcal·mol ⁻¹]						
	KLT(001)	KLT (100)	TiO ₂ (001)	TiO ₂ (100)	TiO ₂ (101)	TiO ₂ (103)	TiO ₂ (112)
Si-O (Ti-O)	579	384	228	300	57	84	172
OH	390	431	625	616	426	404	275

The strongest E_{ad} was obtained for the TiO₂(001)OH surface (2617 kJ·mol⁻¹), followed by TiO₂(100)OH with nearly the same E_{ad} value (2579 kJ·mol⁻¹), leading to the order TiO₂(001)OH ≈ TiO₂(100)OH > KLT(001) > TiO₂(101)OH ≈ KLT(100)OH > TiO₂(103)OH > KLT(001)OH ≈ KLT(100) > TiO₂(100) > TiO₂(112)OH > TiO₂(112) > TiO₂(103) > TiO₂(101). Optimized models of PANI chain on TiO₂(001)OH and TiO₂(100)OH surfaces are shown in Fig. 3. One can see that PANI chain on TiO₂(001)OH and TiO₂(100)OH prefers the directions [110] and [012], respectively. This is caused by the tendency to find a position in which the distances between OH groups (d_{OH-OH}) become similar with the distances between NH groups (d_{NH-NH}) in PANI chains, which are ~ 0.56 nm. For TiO₂(001) and TiO₂(100) planes the d_{OH-OH} in [110] and [012] directions are ~ 0.53 nm and ~ 1.21 nm, respectively. Nearly the same values of d_{OH-OH} in case of [110] direction in TiO₂(001) plane and d_{NH-NH} probably causes slightly stronger interaction between PANI and TiO₂(001)OH

surface than between PANI and $\text{TiO}_2(100)\text{OH}$ surface where the $d_{\text{OH-OH}}$ in case of [012] direction is twice the $d_{\text{NH-NH}}$.

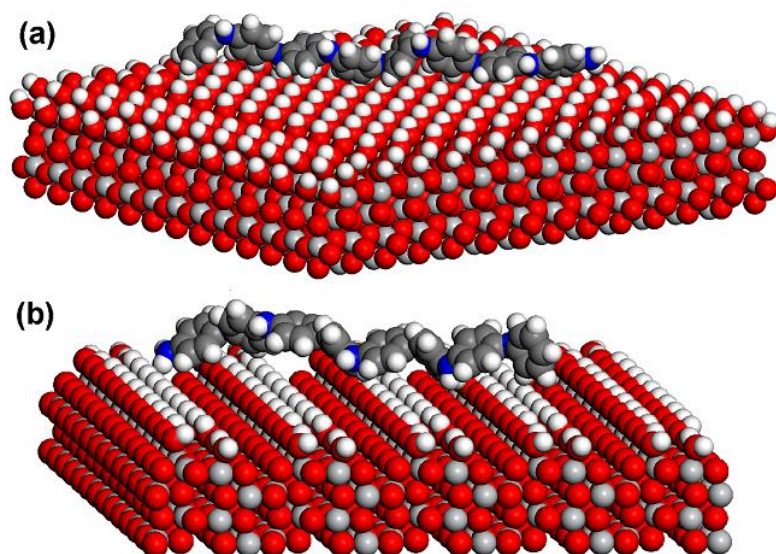


Fig. 3. Optimized models of PANI chain on $\text{TiO}_2(001)\text{OH}$ and $\text{TiO}_2(100)\text{OH}$ surfaces. Ti – light gray, O – red, H – white, C – dark gray, N – blue.

It is evident that PANI interacts preferentially with protonated TiO_2 surfaces, especially with $\text{TiO}_2(001)\text{OH}$ and $\text{TiO}_2(100)\text{OH}$ where the E_{ad} is higher than for KLT. Surprisingly, the interaction of PANI with $\text{KLT}(001)\text{OH}$ surface is weaker than with $\text{KLT}(001)$ and $\text{KLT}(100)\text{OH}$ but nearly the same as with $\text{KLT}(100)$. Although the E_{ad} is lower for $\text{KLT}(001)$ than for $\text{TiO}_2(001)\text{OH}$ and $\text{TiO}_2(100)\text{OH}$, the difference is only about 8 % (see Table 2) and, therefore, PANI can be present on $\text{KLT}(001)$ surface. In PANI/KLT samples the presence of PANI on KLT edges is also possible. The most important finding is that the E_{ad} for $\text{KLT}(100)$ and $\text{KLT}(100)\text{OH}$ do not reach the E_{ad} values for $\text{TiO}_2(001)\text{OH}$ and $\text{TiO}_2(100)\text{OH}$ surfaces. The presence of TiO_2 “collars” on KLT edges in KATI composites causes a more complete coverage by PANI than in case of pure KLT.

The growth of TiO_2 on KLT and the orientation of TiO_2 hkl planes against KLT have been already studied using computer simulations and for our previous results the reader is referred to [33] and [40]. Taking into account the strong adhesions found for $\text{KLT}(100)/\text{TiO}_2(100)$ and $\text{KLT}(100)/\text{TiO}_2(001)$ systems, two of the possible arrangements in PANI/KATI composites can be $\text{KLT}(100) | \text{TiO}_2(100)\text{OH} | \text{PANI}$ and $\text{KLT}(100) | \text{TiO}_2(001)\text{OH} | \text{PANI}$. However, this hypothesis is not supported by experimental analyses.

3.2. Raman spectra

Fig. 4 shows Raman spectra of PANI and TiO_2 in all prepared composites.

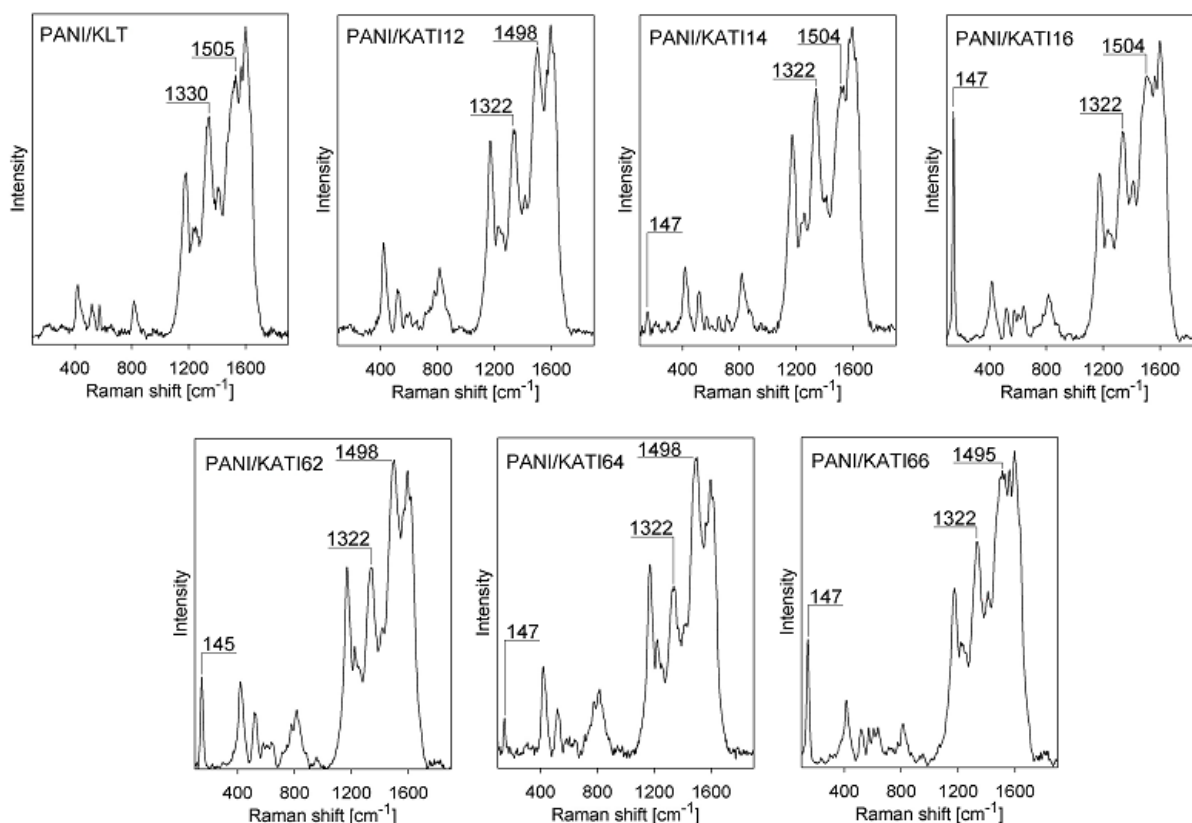


Fig. 4. Raman spectra of prepared PANI/KATI, PANI/KLT and PANI/TiO₂ samples.

KLT substrates (and generally clays) are not visible in Raman spectra due to their fluorescence [41]. TiO₂ (anatase structure) has four main bands [42] but only the strongest one ($\sim 150 \text{ cm}^{-1}$) is detectable in almost all Raman spectra with exception of PANI/KLT and PANI/KATI12 (see Fig. 4). The other bands are not clearly visible due to deformation vibrations of aromatic rings in range $200\text{-}800 \text{ cm}^{-1}$ [43]. Main band of TiO₂ is more or less visible for all calcined samples. For non-calcined samples this band is clearly visible only in the spectrum of PANI/KATI16 containing the highest amount of TiO₂.

The most information about protonation state gave “protonation band” corresponding to C-N⁺ stretching vibration [44]. One can see that this band ($\sim 1320 \text{ cm}^{-1}$) have the highest intensity for sample PANI/KATI14 which corresponds with the highest conductivity (see Table 3). PANI/KATI12 and PANI/KATI62 samples have similar Raman spectra with only small differences in protonation band and band of stretching vibration of $>\text{C}=\text{N}-$ ($\sim 1498 \text{ cm}^{-1}$) [44]. PANI/KATI12 sample exhibits higher protonation band than PANI/KATI62, which is also in good agreement with conductivity of these samples (see Table 3).

3.3. X-ray diffraction analysis

X-ray diffraction (XRD) patterns obtained from various surfaces of tablets (i.e the flat round surface, the outer curved surface and the inner cutting surfaces) pressed from PANI/KLT, PANI/KATI1X and PANI/KATI6X composites are shown in Fig. 5a-c. In addition to the monitored phases kaolinite and anatase (denoted as KLT and A) two other phases quartz and muscovite (denoted as Q and M) have been identified. These minerals are commonly present in raw kaolin clay.

A wide set of low-intensity reflections forming a slight ripple in the range $2\theta = 11\text{--}19^\circ$ (Fig. 5b and c) arises from the longitudinally arranged PANI chains and in ideal case the angle $2\theta \sim 15^\circ$ corresponds to the situation when the planes of aromatic rings in PANI chains are parallel to the direction of pressing (i.e. perpendicular to the diffraction plane). However, no reflection at $2\theta \sim 15^\circ$ can be seen. There is only basal reflection of KLT ($2\theta \sim 14.4^\circ$) which will be discussed later. This suggests that aromatic rings in longitudinally arranged PANI chains are not oriented perpendicular to any diffraction plane, i.e. they are oriented randomly. It is evident that the reason of high anisotropy factors (Table 3) has to be found in the space arrangement of matrices. Platy KLT particles oriented perpendicular to the direction of pressing (i.e. parallel to the flat round surface of tablet, see Fig. 1a) form a barrier limiting the flow of electric current while the conductivity σ_{\perp} in the direction along this flat round surface (see Fig. 1a and Table 3) is significantly higher. One can see that reflections of KLT planes occur in the diffraction patterns obtained both from the flat round surfaces and outer curved surfaces (Figs. 5a and b).

Table 3
Conductivities of pressed tablets. Anisotropy factor $\alpha = \sigma_{\perp} / \sigma_{\parallel}$.

Sample	σ_{\perp} [10^{-5} S/m]	σ_{\parallel} [S/m]	α
PANI/KATI12	1.99	0.72	10^4
PANI/KATI14	4.39	2.76	10^4
PANI/KATI16	0.68	0.01	10^3
PANI/KATI62	2.75	0.22	10^3
PANI/KATI64	9.71	0.18	10^3
PANI/KATI66	3.50	0.03	10^2
PANI/KLT	2.15	0.03	10^3
PANI	16.98	0.03	10^2

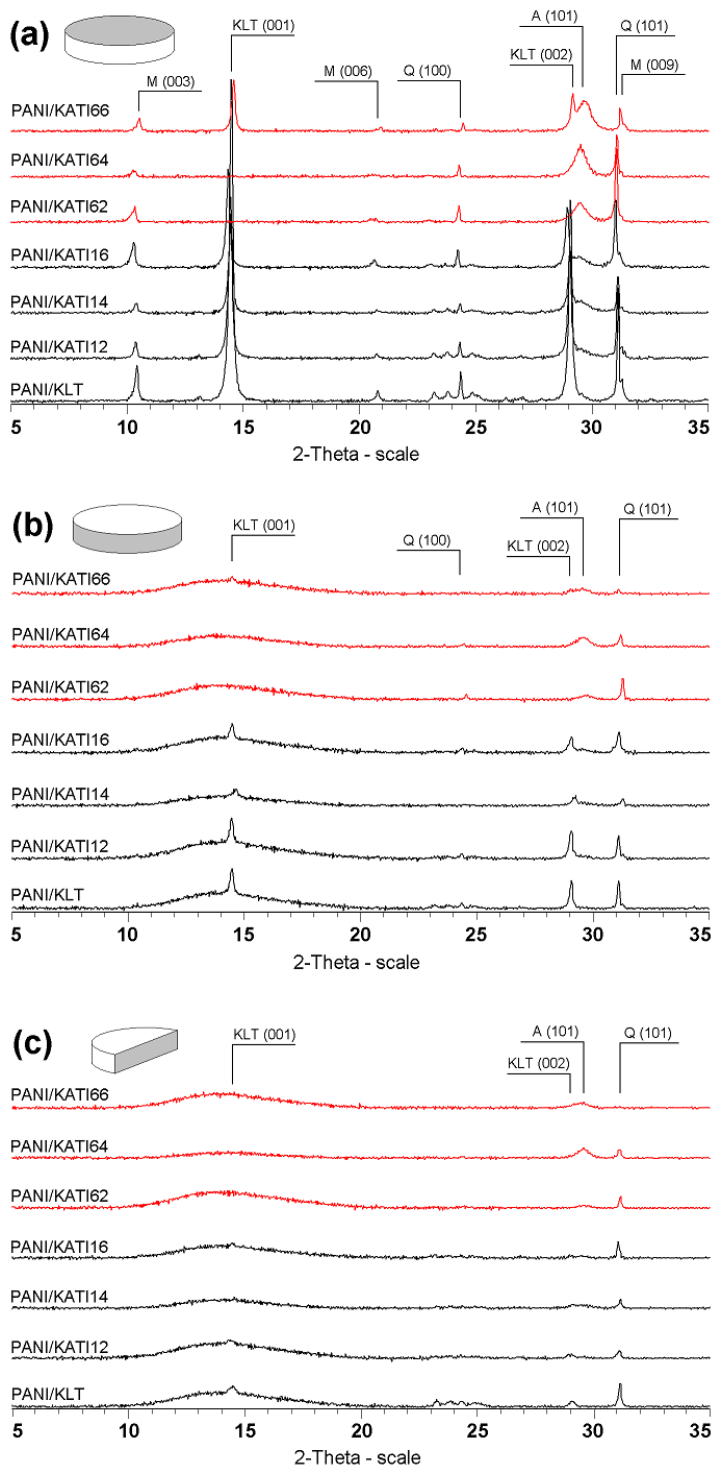


Fig. 5. X-ray diffraction patterns of the flat round surfaces (a); the outer curved surfaces (b); and the inner cutting surfaces (c) for all PANI/KLT and PANI/KATI tablets. The sketches of all three surfaces are also provided. A-anatase, KLT-kaolinite, M-muscovite, Q-quartz.

This is caused by the encountering of KLT and KATI particles with the walls of pressing chamber during the pressing. Because these walls are stationary, the pressure spreading through the powder sample forces the KLT and KATI particles to take the positions parallel to these walls. This does not occur in the internal volume of powder sample and the above

mentioned reflections are not noticeable in the diffractogram of inner cutting surfaces (Fig. 5c).

Although the KLT reflections disappeared in the XRD patterns of PANI/KATI62 and PANI/KATI64, in the XRD pattern of PANI/KATI66 are clearly observable (Fig. 5a) suggesting that the presence of large amount of TiO_2 prevents the full transformation of KLT into metakaolinite. Since the KLT reflections of PANI/KATI66 can be found only in the XRD pattern of the flat round surface, it is probable that their visibility is the result of pressing.

3.4. Conductivity measurement

The in-plane conductivities (σ_{\parallel}), the conductivities in the direction perpendicular to the tablet plane (σ_{\perp}) and the anisotropy factors (α) for all prepared samples are listed in Table 3. One can see that PANI/KATI14 sample exhibits the in-plane conductivity 2.76 S/m which is an order or two orders of magnitude higher than conductivities of other samples. This high conductivity corresponds well with the complete coverage of KATI14 by PANI layer (see Fig. 2e).

Since the exact α values can be affected by an error (due to the very small values σ_{\perp}), only the orders of magnitude are considered. The value α which is of order 10^2 for pure PANI increases due to the addition of KLT and the tablet pressed from PANI/KLT composite exhibits the α of order 10^3 . Moreover, the presence of TiO_2 on KLT further increases the anisotropy and for PANI/KATI12 a PANI/KATI14 the value α is of order 10^4 . This is a maximum value reached for our PANI/KATI composites.

Further, it is evident that using the calcined KATI as a matrix results in the decrease of anisotropy as one can see from the comparison of α for PANI/KATI1X and PANI/KATI6X. This is caused by the partial loss of the KLT layered structure due to the transformation to metakaolinite during calcination. In case of PANI/KATI66 sample the transformation of KLT to metakaolinite is partially inhibited by the presence of large amount of TiO_2 (as mentioned in section 3.3. X-ray diffraction analysis) but, concurrently, this large amount of TiO_2 (i.e. 60 wt.%) causes the decrease of anisotropy (α values for PANI/KATI16 and PANI/KATI66 are lower than for other PANI/KATI samples). PANI/KATI66 exhibits the lowest α value (with exception of pure PANI) because in this sample both the transformation to metakaolinite and the large amount of TiO_2 play its role. In addition, the calcination causes the increasing size of TiO_2 crystallites [33] which may also contribute to the decreasing of α .

The load test results are summarized in Table 4.

Table 4

The values of current obtained during the loading and unloading parts of the measurement. N, m and p represents the number of weights, the load and the pressure, respectively. I (%) shows the value of current (in percentage) relative to the value of current obtained for the highest load.

		PANI/KATI12		PANI/KATI14		PANI/KATI16		PANI/KATI62		
N	m (g)	p (Pa)	I (μA)	I (%)	I (μA)	I (%)	I (μA)	I (%)	I (μA)	I (%)
2	248	3026	510	22.37	23770	113.72	184	45.46	156	25.60
4	496	6052	689	30.20	21501	102.86	241	59.44	219	35.79
6	744	9078	1132	49.62	20209	96.68	297	73.42	330	54.03
8	992	12104	1642	71.96	19856	94.99	330	81.54	434	70.99
10	1240	15130	1954	85.66	20579	98.45	369	91.25	516	84.55
12	1488	18156	2282	100.00	20903	100.00	405	100.00	611	100.00
10	1240	15130	1859	81.49	17719	84.77	356	88.02	515	84.36
8	992	12104	1591	69.74	15084	72.16	315	77.94	441	72.16
6	744	9078	1084	47.50	11617	55.58	273	67.51	354	57.99
4	496	6052	678	29.72	9371	44.83	224	55.30	249	40.77
2	248	3026	332	14.55	6245	29.88	176	43.54	159	26.07

		PANI/KATI64		PANI/KATI66		PANI/KLT		PANI		
N	m (g)	p (Pa)	I (μA)	I (%)	I (μA)	I (%)	I (μA)	I (%)	I (μA)	I (%)
2	248	3026	427	39.28	490	55.37	178	36.04	525	48.38
4	496	6052	542	49.86	578	65.40	236	47.74	622	57.31
6	744	9078	736	67.69	668	75.47	305	61.80	777	71.60
8	992	12104	869	79.90	754	85.23	360	72.83	1041	95.96
10	1240	15130	964	88.69	821	92.78	432	87.42	1045	96.30
12	1488	18156	1087	100.00	885	100.00	494	100.00	1085	100.00
10	1240	15130	951	87.43	815	92.18	428	86.64	967	89.12
8	992	12104	827	76.03	755	85.38	362	73.30	829	76.38
6	744	9078	678	62.35	681	77.03	279	56.49	665	61.35
4	496	6052	510	46.88	587	66.37	206	41.62	441	40.61
2	248	3026	334	30.73	438	49.57	113	22.94	281	25.87

Because the load sensor has to respond to the same external loads identically, special attention has been paid to the values of current obtained for the same load in the loading and unloading part of the measurement. The current (I (μA)) was converted to percent (I (%)) and in order to evaluate the stability of response, differences between both I (%) values for the same load were calculated. An example follows. For 248g load the currents measured on PANI/KATI12 sample were 510 (loading part of the measurement) and 332 μA (unloading part of the measurement), i.e. 22.37 and 14.55 % of the highest current (2282 μA). The difference between these two values is 7.82 %. For the same load the currents measured on PANI/KATI62 sample were 156 and 159 μA, i.e. 25.6 and 26.07 % of the highest current

(611 μA). The difference between these two values is 0.47 %. Although the PANI/KATI62 exhibits lower conductivity, its response to the same load is much more stable.

Table 4 shows that the tablets pressed from PANI/KATI composites exhibit more stable response to the same load than tablets pressed from PANI/KLT and pure PANI. Moreover, it is evident that the responses of samples PANI/KATI6X are more stable than these of samples PANI/KATI1X. The average differences between the values I (%) for the same loads are as follows: 3.53% (PANI/KATI12), 43.9% (PANI/KATI14), 3.76% (PANI/KATI16), 2.15% (PANI/KATI62), 4.40% (PANI/KATI64), 1.82% (PANI/KATI66), 5.16% (PANI/KLT), and 15.24% (PANI).

4. Conclusions

Composites PANI/KATI containing PANI chains on KLT surface modified by nano-TiO₂ has been successfully prepared. Characterization of these composites using X-ray diffraction, scanning electron microscopy, Raman spectroscopy and molecular modeling revealed the arrangement of individual components. The most important finding is the role of TiO₂ which allows PANI to completely cover the surface of KATI particles. Electrical conductivity measurements showed significant anisotropic behavior of PANI/KATI composites. The highest reached anisotropy factor was 10⁴ (PANI/KATI12 and PANI/KATI14) representing an increase of two orders of magnitude compared with PANI and one order of magnitude compared with PANI/KLT. The possibility of using the tablets as load sensors was also tested. It was found that tablets containing dried KATI are not suitable as load sensors, while composites containing calcined KATI seem to be very promising material for this purpose.

Acknowledgement

This research has been funded by the Grant Agency of Czech Republic (project P108/11/1057). Authors wish to thank Tomáš Plaček for his significant assistance in preparation and characterization of the samples.

References

- [1] J. Stejskal, P. Kratochvíl, A.D. Jenkins, *Polymer* 37 (1996) 367-369.
- [2] S. Quillard, G. Louarn, J.P. Buisson, M. Boyer, M. Lapkowski, A. Pron, S. Lefrant, *Synth. Met.* 84 (1997) 805-806.
- [3] Z. Rozlívková, M. Trchová, I. Šeděnková, M. Špírková, J. Stejskal, *Thin Solid Films* 519 (2011) 5933-5941.
- [4] L. Merhari, *Hybrid nanocomposites for Nanotechnology*, first ed. Springer Science + Business Media, LLC, New York, 2009.

- [5] Y.D. Liu, H.J. Choi, *Soft Matter* 8 (2012) 11961-11978.
- [6] K.R. Cromack, M.E. Jozefowicz, J.M. Ginder, A.J. Epstein, R.P. McCall, E. Seherr, A.G. MacDiarmid, *Macromolecules* 24 (1991) 4157-4161.
- [7] A.V. Semakov, A.A. Shabeko, S.G. Kiseleva, A.V. Orlov, A.V. Rebrov, Y.M. Korolev, G.P. Karpacheva, V.N. Kuleznev, V.G. Kulichikhin, *Polym. Sci. B* 52 (2010) 91-100.
- [8] O. Quadrat, J. Stejskal, P. Kratochvíl, C. Klasson, D. McQueen, J. Kubát, P. Sába, *Synth. Met.* 97 (1998) 37-42.
- [9] M. Špírková, J. Stejskal, O. Quadrat, *Synth. Met.* 102 (1999) 1264-1265.
- [10] M. Costolo, A.J. Heeger, *Synth. Met.* 114 (2000) 85-90.
- [11] X. Wu, S. Qi, J. He, G. Duan, *J. Mater. Sci.* 45 (2010) 483-489.
- [12] Y. Cao, P. Smith, A.J. Heeger, *Synth. Met.* 57 (1993) 3514-3519.
- [13] S. Shariki, S.Y. Liew, W. Thielemans, D.A. Walsh, C.Y. Cummings, L. Rassaei, M.J. Wasbrough, K.J. Edler, M.J. Bonne, F. Marken, *J. Solid State Electrochem.* 15 (2011) 2675-2681.
- [14] P.N. Adams, P.J. Laughlin, A.P. Monkman, *Synth. Met.* 76 (1996) 157-160.
- [15] J. Stejskal, M. Špírková, O. Quadrat, P. Kratochvíl, *Polym. Int.* 44 (1997) 283-287.
- [16] F.F. Fang, H.J. Choi, W.S. Ahn, *Compos. Sci. Technol.* 69 (2009) 2088-2092.
- [17] J. Prokeš, M. Varga, I. Křivka, A. Rudajevová, J. Stejskal, *J. Mater. Chem.* 21 (2011) 5038-5045.
- [18] Q. Wu, Z. Xue, Z. Qi, F. Wang, *Polymer* 41 (2000) 2029-2032.
- [19] N.G. Duran, M. Karakısla, L. Aksu, M. Sacak, *Mater. Chem. Phys.* 118 (2009) 93-98.
- [20] S. Yoshimoto, F. Ohashi, Y. Ohnishi, T. Nonami, *Synth. Met.* 145 (2004) 265-270.
- [21] I. Bekri-Abbes, E. Srasra, *Mater. Res. Bull.* 45 (2010) 1941-1947.
- [22] K. Cuentas-Gallegos, M. Lira-Cantú, P. Casañ-Pastor, P. Gómez-Romero, *Adv. Funct. Mater.* 15 (2005) 1125-1133.
- [23] A. Lerf, P. Čapková, in: H.S. Nalva (Ed.) *Encyclopedia of Nanoscience and Nanotechnology*, vol. 2, American Scientific publishers, Stevenson Ranch, CA, USA, 2004, pp. 639-694.
- [24] G. Lagaly, M. Ogawa, I. Dékány, in: F. Bergaya, B.K.G. Theng, G. Lagaly (Eds.), *Handbook of Clay Science, Developments in Clay Science*, vol. 1, Elsevier, Amsterdam, 2006, pp. 309-377.
- [25] M. Ogawa, K. Kuroda, *Chem. Rev.* 95 (1995) 399-438.
- [26] J.C. Hutchison, R. Bissessur, D.F. Shiver, *Chem. Mater.* 8 (1996) 1597-1599.
- [27] S. Kazim, A. Shahzada, J. Pflieger, J. Plestil, Y.M. Joshi, *J. Mater. Sci.* 47 (2012) 420-428.
- [28] M. Oyharcabal, T. Oling, M.-P. Foulc, V. Vigneras, *Synth. Met.* 162 (2012) 555-562.
- [29] P. Bober, J. Stejskal, M. Špírková, M. Trchová, M. Varga, J. Prokeš, *Synth. Met.* 160 (2010) 2596-2604.
- [30] G.M. Do Nascimento, V.R.L. Constantino, R. Landers, M.L.A. Temperini, *Polymer* 47 (2006) 6131-6139.
- [31] D. Anaklı, S. Çetinkaya, *Curr. Appl. Phys.* 10 (2010) 401-406.
- [32] H. Acar, M. Karakısla, M. Sacak, *Mater. Sci. Semicon. Proces.* 16 (2013) 845-850.
- [33] K. Mamulová Kutláková, J. Tokarský, P. Kovář, S. Vojtěšková, A. Kovářová, B. Smetana, J. Kukutschová, P. Čapková, V. Matějka, *J. Hazard. Mater.* 188 (2011) 212-220.
- [34] R.B. Neder, M. Burghammer, T. Grasl, H. Schultz, A. Bram, S. Fiedler, *Clays Clay Miner.* 47 (1999) 487-494.
- [35] C.J. Howard, T.M. Sabine, F. Dickson, *Acta Crystallogr., Sect. B* 47 (1991) 462-468.

- [36] P. Bober, J. Stejskal, M. Špírková, M. Trchová, M. Varga, J. Prokeš, *Synth. Met.* 160 (2010) 2596-2604.
- [37] A.K. Rappe, C.J. Casewit, K.S. Colwell, W.A. Goddard, W.M. Skiff, *J. Am. Chem. Soc.* 114 (1992) 10024-10035.
- [38] J. Gasteiger, M. Marsili, *Tetrahedron* 36 (1980) 3219-3228.
- [39] A.K. Rappe, W.A. Goddard, *J. Phys. Chem.* 95 (1991) 3358-3363.
- [40] J. Tokarský, P. Čapková, J.V. Burda, *J. Mol. Model.* 18 (2012) 2689-2698.
- [41] L.R. Frost, L. Rintoul, *Appl. Clay Sci.* 11 (1996) 171-183.
- [42] S. Srinivasan, A.K. Datye, M.H. Smith, I.E. Wachs, G.B. Deo, J.M. Jehng, A.M. Turek, C.H.F. Pede, *J. Catal.* 131 (1991) 260-275.
- [43] P. Colomban, S. Folch, A. Gruger, *Macromolecules* 32 (1999) 3080-3092.
- [44] S. Quillard, G. Louam, S. Lefrant, A.G. MacDiarmid, *Phys. Rev. B* 50 (1994) 12496-12508.